Conjecturas

DOI: 10.53660/CONJ-1449-2A09

Influence of electrospinning parameters on the morphology and performance of filter media

Influência de parâmetros de *electrospinning* sobre a morfologia e performance de meios filtrantes

Alessandro Estarque de Oliveira[1], Mônica Lopes Aguiar[1], Vádila Giovana Guerra[1]*

ABSTRACT

Nanofibrous filter media used for filtration of nanoparticles dispersed in air can be produced by electrospinning of polymer solutions. However, this process is influenced by many operating variables, including the solution feed conditions. In this work, a 2^3 factorial design was used to evaluate the influence of electrospinning variables on the morphology and performance characteristics of filter media composed of polyvinyl alcohol (PVA) nanofibers. The variables considered were needle-collector distance, collector rotation speed, and spinning time. The dependent variables were the median and geometric standard deviation of the fiber diameter distribution, the overall efficiency for collection of NaCl particles (5.94–224.7 nm), and the initial pressure drop. It was found that the needle-collector distance had the most significant influence on the output variables, especially for the median fiber diameter and the initial pressure drop. For these variables, the fitted curves provided coefficient of determination (R^2) values of 0.98 and 0.96, respectively.

Keywords: Green electrospinning; Air Filtration; Nanofibers; Nanoparticles; Air Pollution Control

RESUMO

Meios filtrantes de nanofibras usados na filtração de nanopartículas dispersas em ar podem ser confeccionados por *electrospinning* de soluções poliméricas. No entanto, este processo está condicionado à influência de inúmeras variáveis operacionais, incluindo condições de alimentação das soluções. Neste trabalho, foi realizado um planejamento fatorial 2^3 para avaliar a influência de variáveis do *electrospinning* sobre características morfológicas e de performance de meios filtrantes de nanofibras de álcool polivinílico (PVA). As variáveis consideradas foram a distância agulha-coletor, a velocidade de rotação do coletor e o tempo de fiação. As variáveis dependentes foram a mediana e o desvio padrão geométrico da distribuição de diâmetro de fibras, a eficiência global de coleta de partículas de NaCl (5,94–224,7 nm) e a queda de pressão inicial. Verificou-se que a distância agulha-coletor foi o parâmetro que afetou mais significativamente as variáveis-resposta, especialmente a mediana e a queda de pressão inicial, cujas curvas de ajuste forneceram valores de coeficientes de determinação (R^2) de 0,98 e 0,96, respectivamente.

Palavras-chave: *Electrospinning* verde; Filtração de Ar; Nanofibras; Nanopartículas; Controle de Poluição do Ar

[1] Universidade Federal de São Carlos.
* E-mail: vadila@ufscar.br

INTRODUCTION

The process of gas cleaning using fibrous filter media consists of an operation of gas-solid separation in which different physical mechanisms act to promote the adhesion of particles to the surfaces of collection agents (the fibers) (TAN, 2014). The efficiencies of these mechanisms (diffusion, interception, electrostatic attraction, gravity, and inertia) are dependent on the particle diameter, among other variables. The collection of nanoparticles is often hindered by their negligible mass (resulting in low efficiencies of the gravitational and inertial mechanisms) and volume (causing low interception efficiency) (TAN, 2014).

One way to enhance the efficiency of nanoparticle filtration is to use nanofibrous filter media. For this purpose, the electrospinning technique is one of the most widely studied processes for the manufacture of nanofibers. This method consists of the passage of a polymeric fluid (polymer solution or melt) through a capillary (or needle) that is connected to a high voltage source. Above a critical voltage, the potential difference generated between the capillary and a collector located at a certain distance is sufficient for the electrical repulsive forces to overcome cohesive forces in the fluid. This results in the formation of a jet that stretches from the Taylor cone formed at the tip of the capillary up to the collector, producing a mat of fibers (OLIVEIRA *et al.*, 2022).

Several variables influence the manufacture of fibers by electrospinning, such as the properties of the polymeric fluid (viscosity, electrical conductivity, and surface tension) and the operating parameters (applied potential difference, distance between the capillary and the collector, capillary inner diameter, fluid flow rate, and rotation speed of the moving collectors, for example). Environmental parameters such as temperature and humidity can also influence this process (RAMAKRISHNA *et al.*, 2005; YARIN *et al.*, 2014). When the nanofibers are used in filter media for air filtration, the filtration performance is not only determined by the morphology of the fibers, but also by factors including the properties of the particulate matter (size, density, and shape), the aerosol concentration, and the velocity of the gas flowing inside the filter medium (TAN, 2014). This means that evaluation and optimization of the characteristics of the filter media are complex, requiring the use of appropriate analysis tools.

In this work, a 2^3 factorial experimental design was used to evaluate the effects of electrospinning parameters on the characteristics of fibers produced using this process, as well as on their performance as filter media in the filtration of nanoparticles dispersed in air. The independent variables evaluated were the needle-collector distance, the rotation speed of the moving collector, and the spinning time. The dependent variables were the median and geometric standard deviation of the fiber diameter distribution, the overall efficiency in the collection of NaCl particles (5.94–224.7 nm), and the initial pressure drop of the filter medium. The polymer used was polyvinyl alcohol (PVA), since it is relatively inexpensive and is soluble in water, so no organic and toxic solvents were required. This meets the nontoxicity and biodegradability requirements of Green Electrospinning (SHI; YANG, 2015; LÓPEZ-CÓRDOBA *et al*., 2016; ZHU *et al*., 2018). The fibers were spun over a cellulose microfibers substrate, which has low efficiency in the collection of nanoparticles, low pressure drop, and provides mechanical strength for the nanofibrous filter medium, as reported previously (OLIVEIRA *et al*., 2021). The aim of this work is to contribute to a better understanding of the effects of different electrospinning parameters on important variables involved in the production of filter media employed in the removal of nanoparticles from air.

METHODOLOGY

Polyvinyl alcohol (molar mass: 104.5 kg/mol; hydrolysis degree: 87.0–89.0% mol) was acquired from Neon (Brazil). Anhydrous citric acid (molar mass: 192 g/mol) was acquired from Synth (Brazil). This component was used to promote the crosslinking of the PVA chains, in order to provide resistance of the fibers to moisture (SHI; YANG, 2015; LÓPEZ-CÓRDOBA *et al.*, 2016). Citric acid also has a low purchase cost and is nontoxic, unlike other crosslinking agents such as the frequently used glutaraldehyde (BOLTO *et al*., 2009). Therefore, this contributed to meeting the requirements of Green Electrospinning.

The cellulose microfibers substrate (PFI 25-24 RAD+, grammage 150 g/m², from Pinus trees) was kindly donated by Ahlstrom-Munksjö (Brazil).

The experimental data were evaluated statistically (using Pareto charts) employing a free trial version of Minitab® 19 software.

The aqueous solution of PVA (13% wt. in relation to the solution mass, as used by Shi and Yang (2015)) was prepared by solubilization of the polymer in deionized water. The mixture was agitated during 1 h, at 80 ºC, under magnetic stirring at 1150 rpm. Citric acid (0.5% wt. in relation to the solution mass) was then added, with stirring for a further 30 min. The solution was left to degas overnight. After the electrospinning of the fibers, the samples were placed in a vacuum oven for 2 h, at 140 ºC, in order to promote the crosslinking, in accordance with the procedure performed by Shi and Yang (2015). Table 1 shows the experimental conditions related to the solution composition, the electrospinning process, and the crosslinking treatment. The highlighted values in Table 1 refer to the conditions varied according to the experimental design described in Table 2. For the rotation speed, the numbers in parentheses are the linear velocities corresponding to the rotation speeds used.

There were no replicates in the fibers production. Therefore, the principle of sparsity was applied (MONTGOMERY; RUNGER, 2014). The suitability of this principle will be proved below.

Table 1 – Nanofibers production parameters

PVA percentage	13% wt. in relation to the solution mass
Citric acid percentage	0.5% wt. in relation to the solution mass
Stirring time	60 min + 30 min with citric acid
Stirring speed	1150 rpm
Stirring temperature	80 ºC
Inner diameter of the needle	0.60 mm
Needle-collector distance	10, 15 cm
Rotation speed of the collector	296, 445 rpm (1.55, 2.33 m/s)
Voltage	27 kV
Spinning time	10, 15 min
Feed flow rate of polymer solution	0.5 mL/h
Oven temperature	140 ºC
Oven time	2 h

Table 2 – Factorial experimental design

Test	Needle-collector distance (cm)	Rotation speed (m/s)	Spinning time (min)
1	10 (-1)	1.55 (-1)	10 (-1)
2	10 (-1)	1.55 (-1)	15 (+1)
3	10 (-1)	2.33 (+1)	10 (-1)
4	10 (-1)	2.33 (+1)	15 (+1)
5	15 (+1)	1.55 (-1)	10 (-1)
6	15 (+1)	1.55 (-1)	15 (+1)
7	15 (+1)	2.33 (+1)	10 (-1)
8	15 (+1)	2.33 (+1)	15 (+1)

Images of the filter media were obtained using a scanning electron microscope (SEM) (FEI Inspect S50) installed in the Structural Characterization Laboratory of the Federal University of São Carlos. The fiber diameters were measured using ImageJ software (RASBAND, 1997–2022).

Samples of each filter medium submitted to the crosslinking treatment, together with untreated samples (Tests 1–8), were immersed in water at room temperature during 24 h, followed by drying for 2 h in a vacuum oven at 50 ºC. The masses of the samples were measured before and after the immersion and drying procedure, using an analytical balance, in order to evaluate any mass losses due to solubilization of the PVA fibers in water.

In the filtration tests, atmospheric air (25 ºC, 92.2 kPa) was fed to the filtration system using a gas compressor, with passage through a set of prefilters to remove humidity and impurities. The compressor of an aerosol generator simultaneously injected previously cleaned atmospheric air into a vessel containing aqueous NaCl solution. The aerosol produced by atomization of the solution then passed through a diffusion dryer to remove the water from the droplets, leaving the salt particles. After drying, the aerosol was mixed with the main air stream exiting the prefilters. Mixing of the air streams occurred immediately after a needle valve used to control the flow rate of the main air stream. The electrical charges of the resultant air stream were neutralized with a charge neutralizer composed of a Kr-85 source. The neutralized aerosol entered a filter holder containing the filter medium with filtering area of ~5.1 cm², which provided a surface velocity of 5.0 cm/s. Aerosol samples were continuously withdrawn from sampling points located before and after the filter holder, subsequently passing through an Am-241 charge neutralizer prior to measurement of the particle concentration with a scanning mobility particle sizer (SMPS). The remaining air stream leaving the filter holder passed through a digital flowmeter located in the exit of the filtration system. The SMPS was connected to a microcomputer for data acquisition. Each aerosol sampling was performed in triplicate, with duration of 315 s for each sample. The sampling flow rate was maintained at 1.5 L/min.

The grade collection efficiency (E_{exp}) was obtained from the concentrations at the inlet (c_e) and outlet (c_s) of the filter, for each diameter measured by the SMPS, as follows:

$$E_{exp}(\%) = \frac{c_e - c_s}{c_e} \times 100 \qquad (1)$$

The grade efficiency was based on the number concentration of particles, which was equivalent to use of a mass basis. Determination of the overall efficiency considered the total concentration of particles on both a number basis and a mass basis. The latter was calculated by the SMPS software, using the particle density and the size distribution of the particles.

The quality factor (q_f) was used to evaluate the performance of the filter media, based on the overall collection efficiency and the pressure drop, as follows (HINDS, 1998):

$$q_f = \frac{-\ln\,(1-E_{exp}(\%)/100)}{\Delta P_0} \qquad (2)$$

where, ΔP_0 is the pressure drop of the clean filter (initial pressure drop). This parameter was obtained with a digital manometer, using the same surface velocity used in the filtration tests, but in the absence of particulate matter.

RESULTS AND DISCUSSION

Figure 1 presents the results of the mass loss tests. The samples submitted to the crosslinking treatment maintained approximately 99.5% of the original masses, even with immersion in water and subsequent drying, while the untreated samples retained less than 98% of the original masses, demonstrating that the crosslinking treatment conferred greater resistance of the fibers to solubilization in water. Analogous results were reported by López-Córdoba *et al*. (2016).

Figure 2 presents SEM images of some samples for illustration and Figure 3 presents the fiber diameter distribution for each sample, including the median and the geometric standard deviation (σ) of each distribution.

Figure 1 – Results of mass losses after immersion in water. The apostrophe indicates treated samples

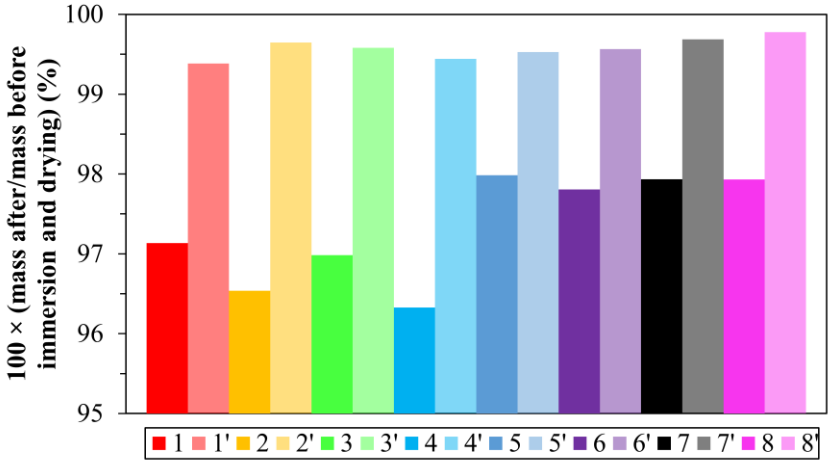

Figure 2 – Images of the surfaces of the filter media 4 (left) and 8 (right). Scale bar: 20 µm

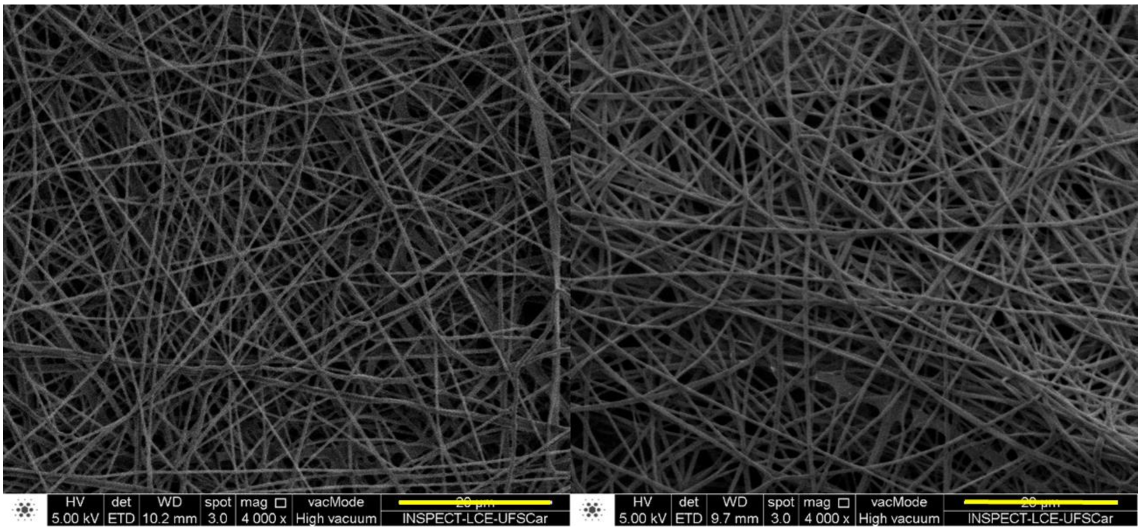

Filtration tests were performed in accordance with the methodology presented before. Therefore, Table 3 presents the results of the dependent variables evaluated: median and σ, overall collection efficiency (mass basis), and initial pressure drop. The overall collection efficiency in number basis and the quality factors in mass and number bases are also presented.

Figure 4 exhibits the particle size distribution used in the filtration tests (a), the grade efficiency curves obtained for each test (b), and the quality factors calculated using Equation 2 (c). The measurements were performed in triplicate and the average values are exhibited.

Table 3 – Morphology and filtration performance parameters

Test	**Median (nm)**	**σ (-)**	**Overall efficiency (mass) (%)**	**Overall efficiency (number) (%)**	**Initial pressure drop (Pa)**	**Quality factor (mass) (Pa^{-1})**	**Quality factor (number) (Pa^{-1})**
1	376	1.28	57.5	71.2	80.5	0.0106	0.0155
2	401	1.64	48.6	60.9	118	0.0057	0.0080
3	398	1.38	55.2	70.0	95.3	0.0084	0.0126
4	413	1.39	78.9	86.7	121	0.0128	0.0166
5	460	1.23	33.9	54.0	46.9	0.0088	0.0166
6	463	1.29	45.8	62.5	66.1	0.0093	0.0148
7	491	1.27	28.0	46.5	50.2	0.0065	0.0125
8	513	1.20	54.9	69.2	59.7	0.0133	0.0197

Figure 3 – Fiber diameter distributions for samples 1(a), 2 (b), 3 (c), 4 (d), 5 (e), 6 (f), 7 (g), and 8 (h)

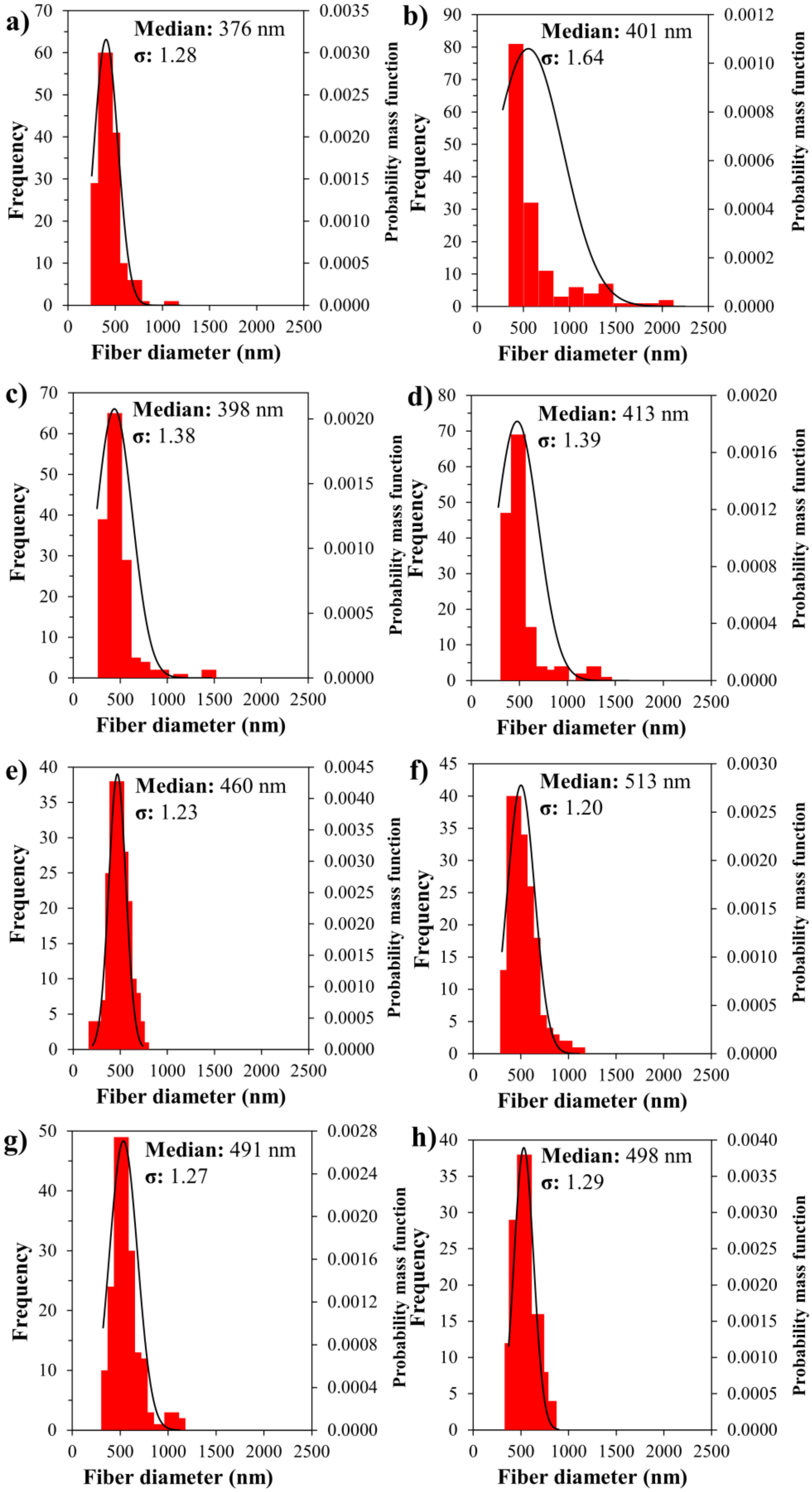

Figure 4 – Size distribution of the particles used in the filtration tests (a), grade efficiency curves (b), and quality factors (c)

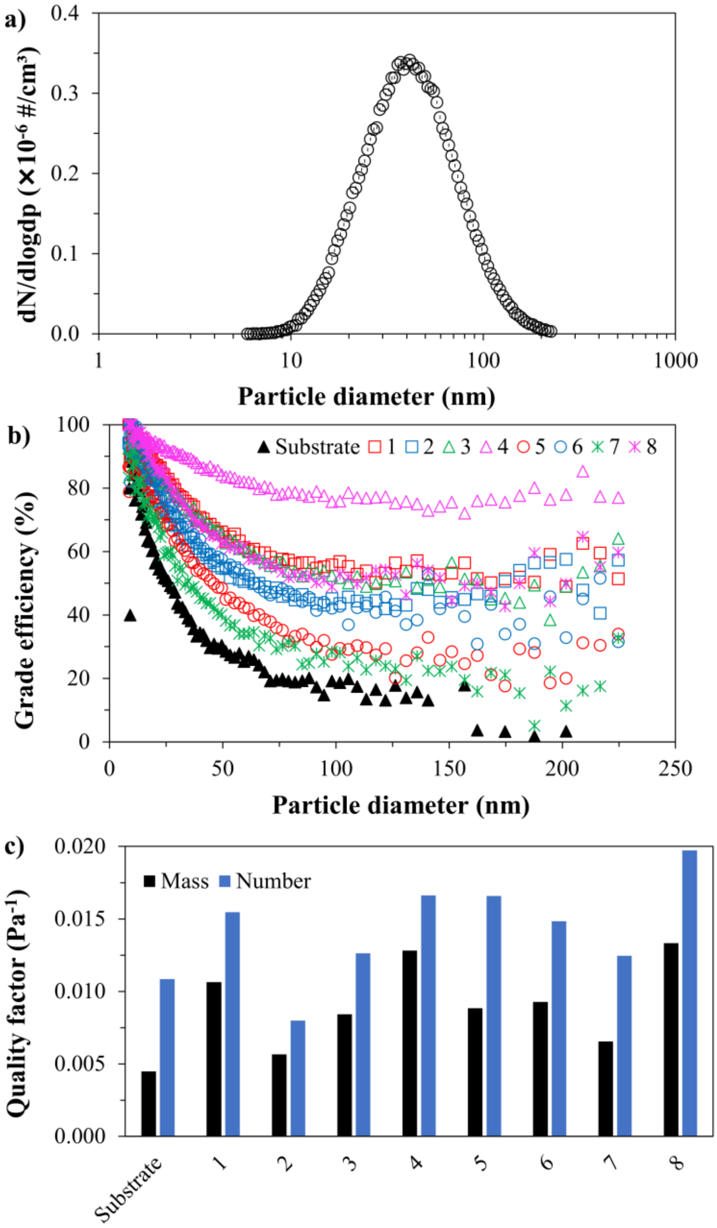

The results (Table 3, Figure 4) showed that increase of the spinning time increased the collection efficiency (tests 3 vs. 4, 5 vs. 6, and 7 vs. 8), except for the pair of samples 1 and 2. Increase of the needle-collector distance decreased the efficiency (tests 1 vs. 5, 3 vs. 7, and 4 vs. 8), except for the pair of samples 2 and 6. The effect of the rotation speed was ambiguous, since for the longest spinning time, increasing the speed favored the efficiency (tests 2 vs. 4 and 6 vs. 8), while the opposite occurred for the shortest spinning time. Condition 4 (shortest distance, highest rotation speed, and longest spinning time) provided the highest grade efficiencies for the entire particle size range. Despite presenting lower efficiency than condition 4, condition 8 provided the highest quality factor (0.0133 Pa^{-1}), followed by condition 4 (0.0128 Pa^{-1}), with both conditions having the longest spinning time and the highest rotation speed. Condition 4 provided the highest pressure drop, which reduced the quality factor (Equation 2), and an analogous interpretation could be made for condition 8.

In general, increasing the spinning time acts to increase of the number of fibers per filtering area, resulting in greater thickness of the filter medium. This increases the collection efficiency, due to greater availability of collection agents, and also increases the resistance to the air flow, which increases the pressure drop (HINDS, 1998). The needle-collector distance is related not only to the strength of the electric field formed when the potential difference is applied, but also to the time available for evaporation of the solvent in the jet after exiting the needle tip (flight time) (TONG; WANG, 2010; ZAKARIA *et al*., 2012; CAO *et al*., 2018). The rotation speed is associated with the alignment of the fibers in the fibrous mat and with a faster rate of solvent evaporation in relation to steady collectors (RAMAKRISHNA *et al*., 2005; MEDEIROS *et al*., 2008).

The data obtained (Table 3) were evaluated statistically using Minitab® software. The Pareto charts for the dependent variables (Figure 5) showed that the needle-collector distance was the most important independent variable affecting the median fiber diameter, followed by the rotation speed and the spinning time. The interaction effects were not significant. In fact, for a significance level of 5%, only the effect of the needle-collector distance was significant, and only for the median fiber diameter and initial pressure drop variables.

For the initial pressure drop and the overall collection efficiency, the effect of the needle-collector distance was most significant, followed by the spinning time. Therefore, the effect of the rotation speed was less significant than some of the combined effects. The effect of the needle-collector distance is related to variations in the electric field and consequently to changes in the electrical forces that lead to the production of fibers, besides association with the time available for evaporation of the solvent. The spinning time is related to the number of fibers spun over the substrate, with its greatest effect being on the initial pressure drop, as discussed above.

Figure 5 – Pareto charts (significance level: 5%) for the median fiber diameter (a), σ (b), overall collection efficiency (c), and initial pressure drop (d), considering the standardized effects of the needle-collector distance (A), rotation speed (B), spinning time (C), and their interactions

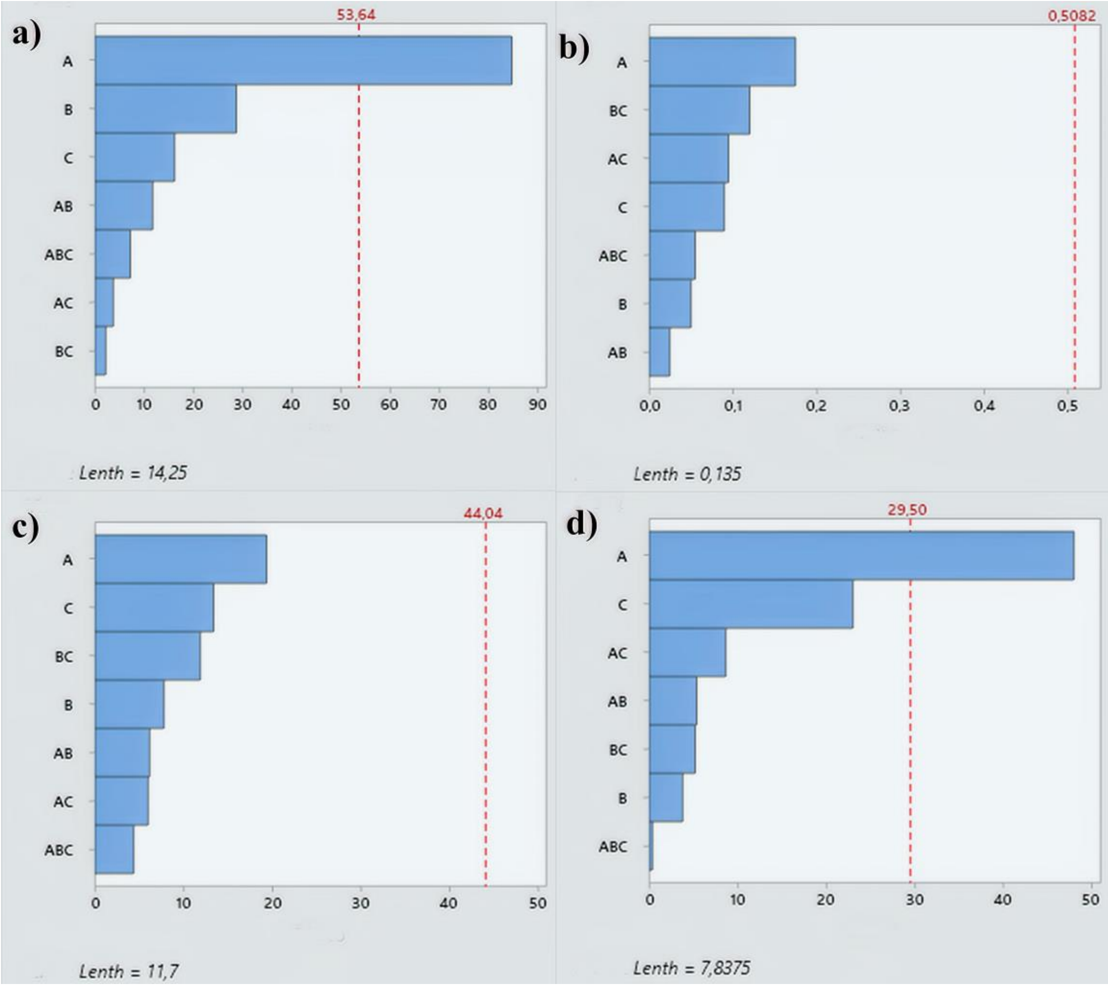

Since the interaction effects were not significant for the range of experimental conditions evaluated for any of the dependent variables, Figure 6 exhibits the main effects plot for each variable.

The results (Figure 6) were consistent with those observed previously, with increase of the needle-collector distance decreasing the collection efficiency and the initial pressure drop, while increasing the spinning time and the rotation speed increased the values of the dependent variables (except for σ). The rotation speed had the weakest effect, under the experimental conditions used. Increase of the needle-collector distance reduced the geometric standard deviation, so the longest distance provided the most homogeneous size distribution. The results for the median fiber diameter showed that weakening of the electric field, due to increase of the distance, led to larger fibers and a more homogeneous fiber mat.

Figure 6 – Main effects plot for the response variables evaluated

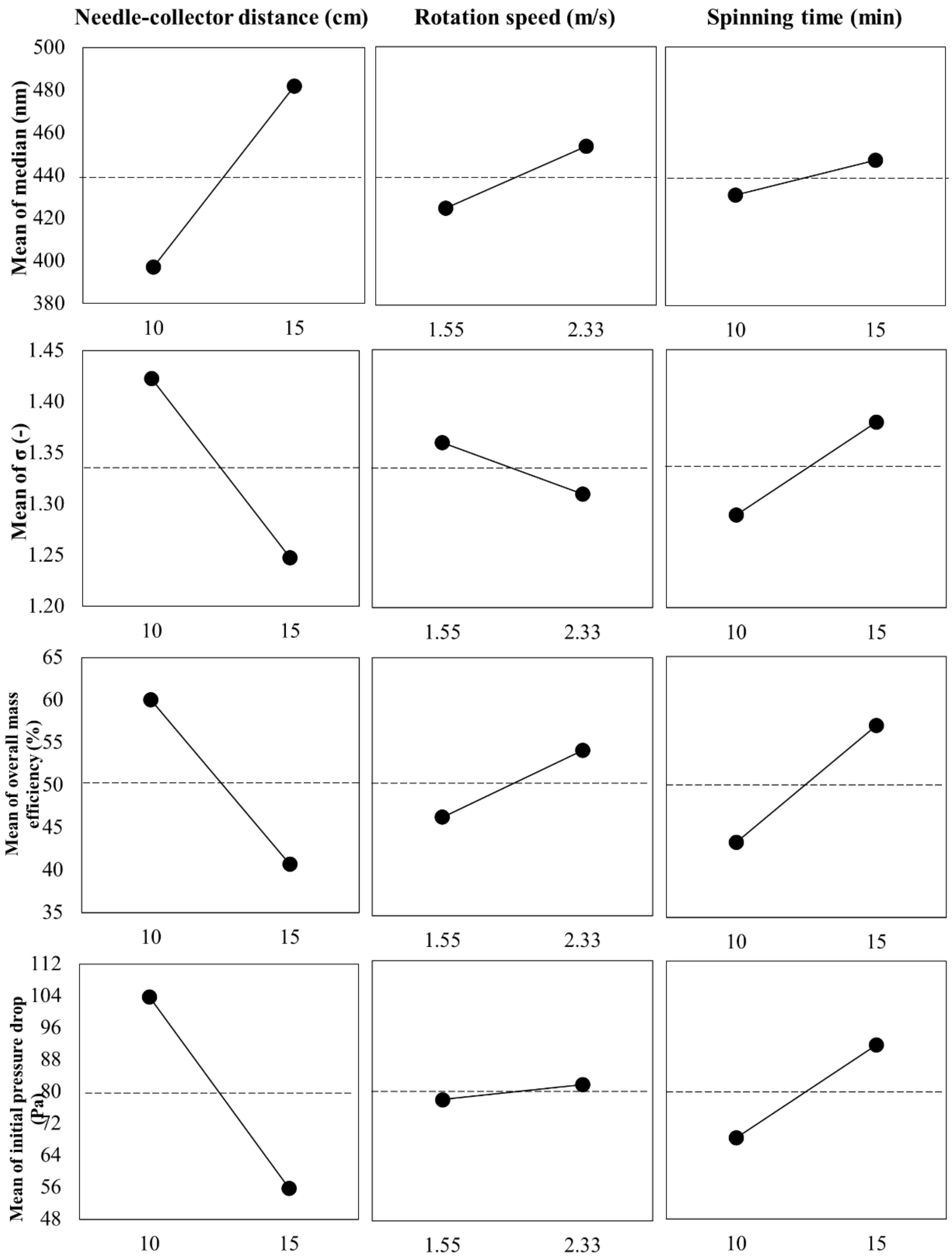

Since the interaction effects were not significant for any of the dependent variables (Figure 5), the application of the sparsity principle could be considered appropriate. According to this principle, in the case of a substantial number of factors, the system is generally dominated by the main effects. Hence, one replicate is usually performed and the higher order interactions can be considered as the error associated with the regression (MONTGOMERY; RUNGER, 2014).

Therefore, Table 4 presents the regression coefficients obtained for the dependent variables, considering only the main effects. Table 5 presents the R^2 values for the fits. Considering the P-values (Table 4), it was evident that the needle-collector distance had the most significant effect for all the response variables evaluated, with P-values below 0.05 for the median and the initial pressure drop, indicating statistical significance for a 95% confidence interval. The coefficients of determination (Table 5) showed that the regression provided better fits of the experimental data for the median fiber diameter and the initial pressure drop.

Table 4 – Regression parameters

	Coefficients	**Standard error**	**P-value**
		Median	
Intercept	115.37	31.51	0.022
Needle-collector distance (cm)	16.95	1.45	0.000
Rotation speed (m/s)	36.86	9.28	0.017
Spinning time (min)	3.25	1.45	0.088
		σ	
Intercept	1.67	0.36	0.010
Needle-collector distance (cm)	-0.04	0.02	0.101
Rotation speed (m/s)	-0.06	0.11	0.576
Spinning time (min)	0.02	0.02	0.335
		Overall mass efficiency	
Intercept	45.95	33.38	0.241
Needle-collector distance (cm)	-3.88	1.53	0.065
Rotation speed (m/s)	10.00	9.84	0.367
Spinning time (min)	2.68	1.53	0.156
		Initial pressure drop	
Intercept	133.07	24.89	0.006
Needle-collector distance (cm)	-9.60	1.14	0.001
Rotation speed (m/s)	4.71	7.33	0.556
Spinning time (min)	4.60	1.14	0.016

Table 5 – Coefficients of determination

	Median	**σ**	**Overall mass efficiency**	**Initial pressure drop**
Multiple R	0.99	0.78	0.85	0.98
R square	0.98	0.60	0.72	0.96
Adjusted R square	0.96	0.31	0.52	0.92
Standard error	10	0.12	11	8.1

Figure 7 presents the results obtained from the regression equations, in comparison with the experimental data. It can be seen that the simulated data were nearer to x = y for the median fiber diameter and the initial pressure drop, compared to the other cases, which was consistent with the data in Table 5.

Figure 7 – Experimental vs. regression results for the median fiber diameter (a), σ (b), overall collection efficiency (c), and initial pressure drop (d)

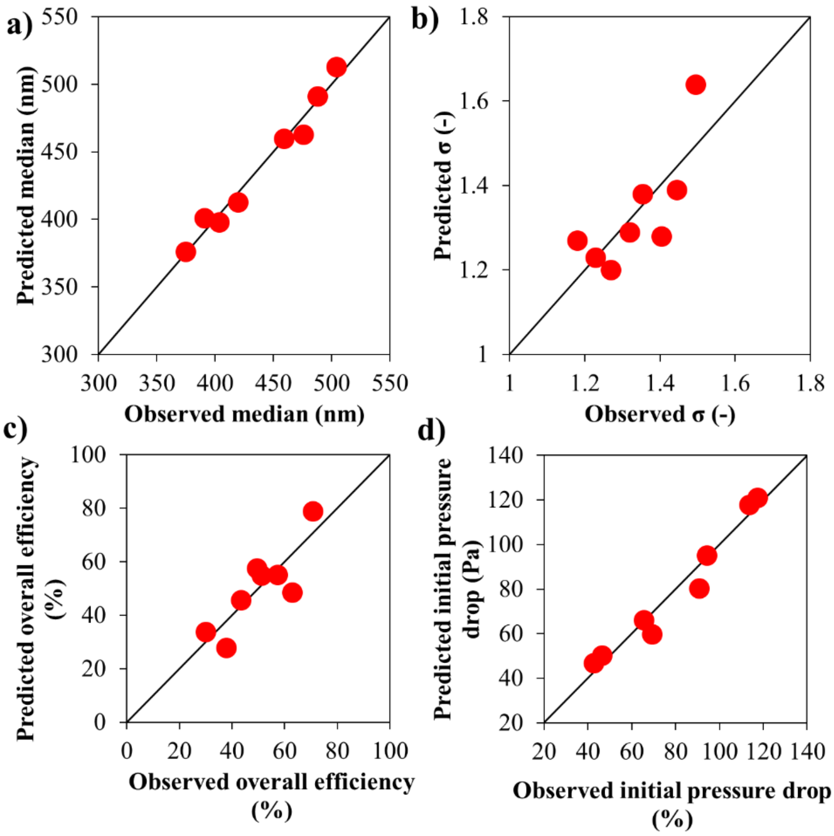

CONCLUSIONS

The methodology adopted in this work enabled evaluation of the effects of different electrospinning operating variables (needle-collector distance, rotation speed, and spinning time) on the morphology and performance parameters of nanofibrous filter media applied in nanofiltration. Under the experimental conditions used, the needle-collector distance had the most significant effect on the response variables, especially the median fiber diameter and the initial pressure drop of the filter medium. The lines of the best fits obtained from the regression of the experimental data provided coefficients of determination (R^2) of 0.98 and 0.96 for the median fiber diameter and the initial pressure drop, respectively.

It must be emphasized that this set of tests was performed using an approach based on a single replicate factorial design, since a high number of independent variables would require a large number of experiments in the case of multiple replicates. It is important to note that electrospinning is influenced by many variables and that consideration of only the three variables evaluated here is not sufficient to fully describe this process. In addition, the response variables related to filtration performance are dependent on other parameters that are specific for the application. Therefore, the number of variables that were maintained constant in this work restricted the present analysis to the experimental conditions employed. Nevertheless, it was possible to identify the strong effect of the needle-collector distance on the dependent variables evaluated, while the range of rotation speeds tested was probably insufficient to cause significant changes in the response variables. Therefore, further studies with wider ranges of rotation speeds are recommended for more detailed analysis of the influence of this operating condition on the response variables.

ACKNOWLEDGEMENTS

The authors are grateful for the financial support provided by CNPq (141299/2019-3) and CAPES (001). The authors also thank the Laboratory of Structural Characterization (LCE/DEMa/UFSCar) for the provision of general facilities, and Ahlstrom-Munksjö (Brazil) for supplying the cellulose filter media used in the tests.

REFERENCES

BOLTO, B.; TRAN, T.; HOANG, M.; XIE, Z. **Crosslinked poly(vinyl alcohol) membranes.** Progress in Polymer Science, vol. 34, p. 969 – 981, 2009. https://doi.org/10.1016/j.progpolymsci.2009.05.003.

CAO, D.; SHI, Y.; FU, Z.; LI, X.; YANG, L.; YAN, D. **Controllable fabrication of micro/nanostructures by electrospinning from polystyrene/poly(vinyl alcohol) emulsion dispersions.** Journal of Applied Polymer Science, vol. 135, n. 26, 46288, 2018. https://doi.org/10.1002/app.46288.

HINDS, C. W. **Aerosol Technology:** Properties, Behaviour, and Measurement of Airborne Particles, 2ª ed. New York: John Wiley, 1998.

LÓPEZ-CÓRDOBA, A.; CASTRO, G. R.; GOYANES, S. **A simple green route to obtain poly(vinyl alcohol) electrospun mats with improved water stability for use as

potential carriers of drugs. Materials Science and Engineering C, vol. 69, p. 726 – 732, 2016. https://doi.org/10.1016/j.msec.2016.07.058.

MEDEIROS, E. S.; MATTOSO, L. H. C.; ITO, E. N.; GREGORSKI, K. S.; ROBERTSON, G. H.; OFFEMAN, R. D.; WOOD, D. F.; ORTS, W. J.; IMAM, S. H. **Electrospun Nanofibers of Poly(vinyl alcohol) Reinforced with Cellulose Nanofibrils**. Journal of Biobased Materials and Bioenergy, vol. 2, n. 3, p. 231 – 242, 2008. https://doi.org/10.1166/jbmb.2008.411.

MONTGOMERY, D. C.; RUNGER, G. C. **Applied statistics and probability for engineers**. 6ª ed. Hoboken: Wiley, 2014.

OLIVEIRA, A. E.; AGUIAR, M. L.; GUERRA, V. G. **Theoretical Analysis of Air Filtration Phenomena for a Micro-Fibrous Filter Medium Enhanced with Electrospun Nanofibres**. Aerosol Science and Engineering, vol. 5, p. 81–92, 2021. https://doi.org/10.1007/s41810-020-00086-y.

OLIVEIRA, A. E.; BONFIM, D. P. F.; SALUSSOGLIA, A. I. P.; MEDEIROS, G. B.; GUERRA, V. G.; AGUIAR, M. L. Nanofiber Production Techniques Applied to Filtration Processes. In: HUSSAIN, C. M.; COSTA, G. M. **Environmental, Ethical, and Economical Issues of Nanotechnology**. New York: Jenny Stanford, 2022. p. 31–60. https://doi.org/10.1201/9781003261858-2.

RAMAKRISHNA, S.; FUJIHARA, K.; TEO, W.-E-.; LIM, T.-C.; MA, Z. Electrospinning Process. In: ______. **An Introduction to Electrospinning and Nanofibers**. New Jersey: World Scientific. Hoboken: John Wiley & Sons, 2005. p. 90 – 154.

RASBAND, W. S. **ImageJ.** U. S. National Institutes of Health, Bethesda, Maryland, USA, <https://imagej.nih.gov/ij/>, 1997-2022.

SHI, J.; YANG, E. **Green electrospinning and crosslinking of polyvinyl alcohol/ citric acid.** Journal of Nanoparticle Research, vol. 32, p. 32 – 42, 2015. https://doi.org/10.4028/www.scientific.net/JNanoR.32.32.

TAN, Z. **Air Pollution and Greenhouse Gases:** From Basic Concepts to Engineering Applications for Air Emission Control. Singapore: Springer, 2014.

TONG, H.-W.; WANG, M. **Electrospinning of fibrous polymer scaffolds using positive voltage or negative voltage:** a comparative study. Biomedical Materials, vol. 5, 054110, 2010. https://doi.org/10.1088/1748-6041/5/5/054110.

YARIN, A. L.; POURDEYHIMI, B.; RAMAKRISHNA, S. General quasi-one-dimensional equations of dynamics of free liquid jets, capillary and bending instability. In: ______. **Fundamentals and Applications of Micro- and Nanofibers.** New York: Cambridge University Press, 2014. p. 63 – 88.

ZAKARIA, S. M.; ZEIN, S. H. S.; OTHMAN, M. R.; JANSEN, J. A. **Hydroxyapatite nanoparticles:** Electrospinning and calcination of hydroxyapatite/polyvinyl butyral nanofibers and growth kinetics. Journal of Biomedical Materials Research, vol. 101A, p. 1977 – 1985, 2012. https://doi.org/10.1002/jbm.a.34506.

ZHU, M.; HUA, D.; PAN, H.; WANG, F.; MANSHIAN, B.; SOENEN, S. J.; XIONG, R.; HUANG, C. **Green electrospun and crosslinked poly(vinyl alcohol)/poly(acrylic acid) composite membranes for antibacterial effective air filtration.** Journal of Colloid and Interface Science, vol. 511, p. 411 – 423, 2018. https://doi.org/10.1016/j.jcis.2017.09.101.

Recebido em: 06/07/2022

Aprovado em: 12/08/2022

Publicado em: 18/08/2022